Influence of uniform blowing/suction on the free convection of non-Newtonian fluids over a vertical plate in porous media with internal heat generation and Soret/Dufour effects

Chuo-Jeng Huang
Email: hcj631216@yahoo.com.tw
Department of Aircraft Engineering, Air Force Institute of Technology, Taiwan (R.O.C.)

ABSTRACT

A non-similarity solution is proposed for the analysis of uniform blowing/suction influence of the steady free convection boundary layers over a vertical plate embedded in a non-Newtonian fluid saturated porous medium with internal heat generation and Soret/Dufour effects. The heat and mass transfer characteristics due to the influence of uniform blowing/suction are numerically analyzed. The surface of the vertical plate has a uniform wall temperature and uniform wall concentration (UWT/UWC). The transformed governing equations are solved by Keller box method. Comparisons showed excellent agreement with the numerical data in previous works. Numerical data for the dimensionless temperature profile, the dimensionless concentration profile, the local Nusselt number and the local Sherwood number are presented for the main parameters: the power-law index of the non-Newtonian fluid n, the blowing/suction parameter ξ and internal heat generation coefficient A^*.

Keywords：uniform blowing/suction, non-Newtonian fluid, Soret/Dufour effects, internal heat generation, free convection, vertical plate, porous media

1. Introduction

Due to various applications of convective heat transfer in porous media it has received great importance during the last decades. Areas of application include the insulation of buildings and equipments, energy storage and recovery, geothermal reservoirs, geophysical engineering, nuclear waste disposal, chemical reactor engineering and the storage of heat generating materials such as grain and coal. In addition, the increase in the recently production of heavy crude oils, and elsewhere where materials whose flow behavior in shear cannot be characterized by Newtonian relationships, it has become necessary to have an adequate understanding of the archeological effects of non-Newtonian fluid flows and, as a result, a new stage in the evolution of fluid dynamic theory is in progress. Nield and Bejan [1] recently provide a comprehensive account of the available information in the field.

In particular, a number of industrially important fluids including fossil fuels exhibit non-Newtonian fluid behavior. Non-Newtonian power law fluids are so widespread in industrial processes and in the environment that it would be no exaggeration to affirm that Newtonian shear flows are the exception rather than the rule. In the aspect of pure heat transfer, Chen and Chen [2] presented similarity solutions for natural convection of a non-Newtonian fluid over vertical surfaces in porous media. In the aspect of coupled heat and mass transfer, the double-diffusion from a

vertical surface in a porous region saturated with a non-Newtonian fluid has been treated by Rastogi and Poulikakos [3]. Jumah and Mujumdar [4] examined the natural convection heat and mass transfer from a vertical plate with variable wall temperature and concentration to power-law fluids with yield stress in a porous medium. Cheng [5] studied the natural convection heat and mass transfer of non-Newtonian power law fluids with yield stress in porous media from a vertical plate with variable wall heat and mass fluxes. Tai and Char [6] investigated the Soret and Dufour effects on free convection flow of non-Newtonian fluids along a vertical plate embedded in a porous medium with thermal radiation. Bagai and Nishad [7] presented the free convection in a non-Newtonian fluid along a horizontal plate embedded in porous media with internal heat generation

The effect of internal heat generation has several important applications, including reactor safety analyses, metal waste form development for spent nuclear fuel, fire and combustion studies, and radioactive materials storage. A new class of similarity solutions was obtained for an isothermal vertical plate in a semi-infinite quiescent fluid with internal heat generation decaying exponentially by Crepeau and Clarksean [8]. Postelnicu and Pop [9] then used the model developed by Crepeau and Clarksean [8] to study the similarity solutions of free convection boundary layers over vertical and horizontal surfaces in porous media with internal heat generation. Grosan and Pop [10] extended the work of Chen and Chen [2] to obtain a free convection over a vertical flat plate with a variable wall temperature and internal heat generation in a porous medium saturated with a non-Newtonian fluid. Grosan et al. [11] described the free convection boundary layer over a vertical cone in a non-Newtonian fluid saturated porous medium with internal heat generation. Patil et al. [12] described a flow and heat transfer over a moving vertical plate in a parallel free stream role of internal heat generation or absorption. Yih and Huang [13] extended the research of Grosan and Pop [10] to report the effect of internal heat generation on free convection heat and mass transfer of non-Newtonian fluids flow over a vertical plate in porous media with variable wall temperature and concentration. Yih and Huang [14] studied the effect of internal heat generation on free convection flow of non-Newtonian fluids over a vertical truncated cone in porous media: VWT/VWC.

However, in the above papers [3–14], these scholars are concentrated upon the impermeable case. Minkowycz and Cheng [15] reported local non-similar solutions for free convective flow with uniform lateral mass flux in porous medium. Hooper et al. [16] investigated the mixed convection from a vertical plate in porous media with surface injection or suction. Yang and Wang [17] investigated the natural convection heat transfer of non-Newtonian power-law fluids with yield stress over axisymmetric and two-dimensional bodies of arbitrary shape embedded in a fluid-saturated porous medium. Yih [18] examined the effect of uniform lateral mass flux on free convection about a vertical cone embedded in a saturated porous medium. Yih [19] investigate the effect of uniform lateral mass flux on the heat transfer characteristics by natural convection of non-Newtonian fluids over a cone in a saturated porous medium. Ibrahim et al. [20] reported the radiative and thermal dispersion effects on non-Darcy natural convection with lateral mass flux for non-Newtonian fluid from a vertical flat plate in a saturated porous medium. Ail [21] investigated

the effect of a heated vertical plate embedded in a saturated porous medium with internal heat generation. Chamkha and Ben-Nakhi [22] studied the MHD mixed convection–radiation interaction along a permeable surface immersed in a porous medium in the presence of Soret and Dufour's effects. Kumari and Nath [23] studied natural convection from a vertical cone in a porous medium due to the combined effects of heat and mass diffusion with non-uniform wall temperature/concentration or heat/mass flux and suction/injection. Rashad et al. [24] examined natural convection boundary layer of a non-Newtonian fluid about a permeable vertical cone embedded in a porous medium saturated with a nanofluid.

The present work extends the work of Yih and Huang [12] by investigating the heat and mass transfer by free convection of non-Newtonian fluids flow over a vertical permeable flat plate under uniform wall temperature and uniform wall concentration (UWT/UWC) embedded in porous media considering the Soret and Dufour effects with internal heat generation.

2. Analysis

The considered problem is the influence of uniform blowing/suction on the natural convection of non-Newtonian fluids over a vertical plate in porous media with internal heat generation and Soret/Dufour effects and where the boundary condition is uniform wall temperature T_w and uniform wall concentration C_w (UWT/UWC), respectively. Fig. 1 shows the flow model and physical coordinate system. The origin of the coordinate system is the leading edge of the vertical flat plate, where x and y are Cartesian coordinates for the distance along and normal to, respectively, the vertical flat plate surface.

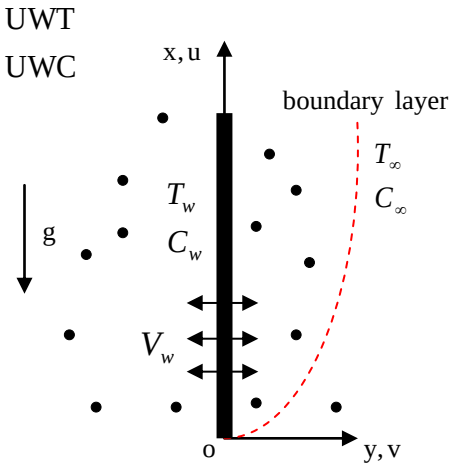

Fig. 1 The flow model and the physical coordinate system

All the fluid properties are assumed to be constant except for the density variation in the buoyancy term. Introducing the boundary layer approximation, the governing equations and the boundary conditions based on the Darcy law can be written as follows:

Continuity equation:

$$\frac{\partial u}{\partial x}+\frac{\partial v}{\partial y}=0 \tag{1}$$

Momentum (Darcy) equation:

$$u^n=-\frac{K(n)}{\mu}\left(\frac{\partial p}{\partial x}+\rho g\right) \tag{2}$$

$$v^n=-\frac{K(n)}{\mu}\left(\frac{\partial p}{\partial y}\right) \tag{3}$$

Energy equation:

$$u\frac{\partial T}{\partial x}+v\frac{\partial T}{\partial y}=\alpha_m\frac{\partial^2 T}{\partial y^2}+\overline{D}\frac{\partial^2 C}{\partial y^2}+\frac{q'''}{\rho c} \tag{4}$$

Concentration equation:

$$u\frac{\partial C}{\partial x}+v\frac{\partial C}{\partial y}=D_M\frac{\partial^2 C}{\partial y^2}+\overline{S}\frac{\partial^2 T}{\partial y^2} \tag{5}$$

Boussinesq approximation:

$$\rho=\rho_\infty\left[1-\beta_T\left(T-T_\infty\right)-\beta_C\left(C-C_\infty\right)\right] \tag{6}$$

Boundary conditions:

$$y=0:\ v=V_w,\ T=T_w,\ C=C_w \tag{7}$$

$$y\to\infty:\ u=0,\ T=T_\infty,\ C=C_\infty \tag{8}$$

Here, u and v are the Darcian velocities in the x- and y- directions, respectively; n is the power-law index of the non-Newtonian fluid; $K(n)$ is the permeability of the porous medium; g is the gravitational acceleration; p, ρ, and μ are the pressure, the density and the absolute viscosity, respectively; T and C are the volume-averaged temperature and concentration, respectively; α_m and D_M are the equivalent thermal diffusivity and mass diffusivity, respectively; $\overline{D}$ and $\overline{S}$ are the Dufour coefficient and Soret coefficients of the porous medium, respectively; β_T and β_C are the thermal and concentration expansion coefficients of the fluid, respectively; V_w is the uniform blowing/suction velocity.

The power-law fluid index n for various fluids is as follows:

(i) $n<1$ for pseudo-plastic fluids (for example, the polymer solution) or shear-thinning fluids that have a lower apparent viscosity at higher shear rates.

(ii) $n=1$ for Newtonian fluids (for instance, air and water) where the shear stress is directly proportional to the shear rate.

(iii) $n>1$ for dilatant fluids (for example, the suspensions of sand) or shear-thickening fluids for which there is an increase in the apparent viscosity at higher shear rates.

For the power law model of Ostwald-de-Waele, Christopher and Middleman [25] and Dharmadhikari and Kale [26] proposed the following relationships for the permeability:

$$K(n)=\begin{cases}\dfrac{6}{25}\left(\dfrac{n\varepsilon}{3n+1}\right)^{n}\left[\dfrac{\varepsilon d}{3(1-\varepsilon)}\right]^{n+1} & [25]\\ \dfrac{2}{\varepsilon}\left[\dfrac{d\varepsilon^{2}}{8(1-\varepsilon)}\right]^{n+1}\left(\dfrac{6n+1}{10n-3}\right)\left(\dfrac{16}{75}\right)^{\frac{3(10n-3)}{(10n+1)}} & [26]\end{cases} \tag{9}$$

where d is the particle diameter while ε is the porosity.

The stream function ψ is defined by

$$u=\partial\psi/\partial y \quad \text{and} \quad v=-\partial\psi/\partial x \tag{10}$$

Therefore, the continuity equation is automatically satisfied.

Next consider the governing Eqs. (2) and (3). Cross-differentiation $\partial(u^n)/\partial y-\partial(v^n)/\partial x$, eliminates the pressure terms in Eqs. (2) and (3). Further, by using the boundary layer approximation $(\partial/\partial x<<\partial/\partial y, v<<u)$,

$$\frac{\partial u^{n}}{\partial y}=\frac{\rho_{\infty}gK(n)}{\mu}\left(\beta_{T}\frac{\partial T}{\partial y}+\beta_{C}\frac{\partial C}{\partial y}\right) \tag{11}$$

Integrating equation (11) once and with the aid of equation (8),

$$u^{n}=\frac{\rho_{\infty}gK(n)}{\mu}\left[\beta_{T}(T-T_{\infty})+\beta_{C}(C-C_{\infty})\right] \tag{12}$$

The second and third terms on the right-hand side of the energy Eq. (4) represent the Dufour effect and the heat absorbed per unit volume, and the last term of concentration Eq. (5) denotes the Soret effect.

The following dimensionless variables are invoked:

$$\xi=\frac{2V_{w}x}{\alpha Ra_{x}^{1/2n}} \tag{13.1}$$

$$\eta=\frac{y}{x}Ra_{x}^{1/2n} \tag{13.2}$$

$$f(\xi,\eta)=\frac{\psi}{\alpha Ra_{x}^{1/2n}} \tag{13.3}$$

$$\theta(\xi,\eta)=\frac{T-T_{\infty}}{T_{w}-T_{\infty}} \tag{13.4}$$

$$\phi(\xi,\eta)=\frac{C-C_\infty}{C_w-C_\infty} \tag{13.5}$$

$$Ra_x=\frac{\rho_\infty g\beta_T\left[T_w-T_\infty\right]\,K(n)}{\mu}\left(\frac{x}{\alpha}\right)^n \tag{13.6}$$

where Ra_x is the local Rayleigh number.

The internal heat generation rate per unit volume q''' is modeled according to the following equation [8–14]:

$$q'''=A^*\cdot\frac{k\left(T_w-T_\infty\right)}{x^2}\cdot Ra_x^{1/n}\cdot e^{-\eta} \tag{14}$$

Here, k is the equivalent thermal conductivity of porous medium; A^* is the internal heat generation coefficient. Note that when $A^*=0$ corresponds to the case 1: no internal heat generation; while for $A^*>0$ corresponds to the case 2: with internal heat generation.

Substituting Eqs. (13)-(14) into Eqs. (12), (4)-(5), (7)-(8) obtains

$$\left(f'\right)^n=\theta+N\phi \tag{15}$$

$$\theta''+\frac{1}{2}f\theta'+D\phi''+A^*\cdot e^{-\eta}=\frac{1}{2}\xi\left(f'\frac{\partial\theta}{\partial\xi}-\theta'\frac{\partial f}{\partial\xi}\right) \tag{16}$$

$$\frac{1}{Le}\phi''+\frac{1}{2}f\phi'+S\theta''=\frac{1}{2}\xi\left(f'\frac{\partial\phi}{\partial\xi}-\phi'\frac{\partial f}{\partial\xi}\right) \tag{17}$$

The boundary conditions are defined as follows:

$$\eta=0:\quad f=-\frac{\xi}{2},\quad \theta=1,\quad \phi=1 \tag{18}$$

$$\eta\to\infty:\qquad \theta=0,\qquad \phi=0 \tag{19}$$

For the new variables, the Darcian velocities in the x- and y- directions are also respectively obtained by

$$u=\frac{\alpha Ra_x^{1/n}}{x}f' \tag{20}$$

$$v = -\frac{\alpha Ra_x^{1/2n}}{2x}\left[f + \xi \frac{\partial f}{\partial \xi} - \eta f' \right] \tag{21}$$

where primes denote differentiation with respect to η. ξ defined in Eq. (13.1) is the surface blowing/suction parameter; Eq. (18.1) can be obtained by integrating Eq. (21) versus ξ once and by setting $\eta = 0$ (at the surface, $y = 0$, then $\eta = 0$), and with the help of boundary Eq. (7). On the one hand, for the case of blowing, $V_w > 0$ and hence $\xi > 0$. On the other hand, for the case of suction, $V_w < 0$ and hence $\xi < 0$. Besides, the buoyancy ratio N, the Lewis number Le, the Dufour parameter D and the Soret parameter S are respectively defined as follows:

$$N = \frac{\beta_C [C_w - C_\infty]}{\beta_T [T_w - T_\infty]}, \qquad Le = \frac{\alpha}{D_M} \tag{22}$$

$$D = \frac{\overline{D}[C_w - C_\infty]}{\alpha [T_w - T_\infty]}, \qquad S = \frac{\overline{S}[T_w - T_\infty]}{\alpha [C_w - C_\infty]} \tag{23}$$

The results for heat and mass transfer rates have practical applications. The heat and mass transfer rates are expressed in terms of the local Nusselt number Nu_x and the local Sherwood number Sh_x, which are respectively defined as follows:

$$Nu_x = \frac{h_x x}{k} = \frac{q_w x}{[T_w - T_\infty]k} = \frac{-\left(\frac{\partial T}{\partial y}\right)\Big|_{y=0} x}{[T_w - T_\infty]k} \tag{24}$$

$$Sh_x = \frac{h_{m,x} x}{D_M} = \frac{m_w x}{[C_w - C_\infty]D_M} = \frac{-\left(\frac{\partial C}{\partial y}\right)\Big|_{y=0} x}{[C_w - C_\infty]D_M} \tag{25}$$

By applying Eq. (13), the local Nusselt number Nu_x and the local Sherwood number Sh_x in terms of $Ra_x^{1/2n}$ are respectively obtained by

$$\frac{Nu_x}{Ra_x^{1/2n}} = -\theta'(\xi, 0) \tag{26}$$

$$\frac{Sh_x}{Ra_x^{1/2n}} = -\phi'(\xi, 0) \tag{27}$$

It may be noticed that for $D = S = 0$, $\xi = 0$ (without blowing/suction effect), Eqs. (15)-(19) are reduced to those of Yih and Huang [12] where a similar solution was obtained previously.

3. Numerical Method

The present analysis integrates the system of Eqs. (15)-(19) by the implicit finite difference approximation together with the modified Keller box method of Cebeci and Bradshaw [27]. First, the partial differential equations converted into a system of five first-order equations. These first-order equations are then expressed in finite difference forms and solved along with their boundary conditions by applying an iterative scheme. This approach improves the convergence rate and the computation times.

Computations were performed with a personal computer with the first step size $\Delta\xi = 0.1$ and $\Delta\eta_l = 0.01$. The variable grid parameter is chosen 1.01 and the value of $\eta_\infty = 30$. The iterative procedure is stopped to give the final temperature and concentration distributions when the error in computing the θ'_w and ϕ'_w in the next procedure becomes less than 10^{-5}.

4. Results and Discussion

The accuracy of this method was verified by comparing the results with those of Tai and Char [6], Grosan and Pop [10], Yih and Huang [12], Yih and Huang [13], Minkowycz and Cheng [15], Hooper et al. [16], Yih [18], Yih [19], Chamkha and Ben-Nakhi [22] and Postelnicu [28]. Table 1 lists the comparison of $-\theta'(\xi,0)$ for various values of ξ with $N = D = S = A^* = 0, n = 1$. Table 2 lists the comparison of $-\theta'(\xi,0)$ for various values of n and ξ with $N = D = S = A^* = 0$. Table 3 lists the comparison of $-\theta'(\xi,0)$ and $-\phi'(\xi,0)$ for various values of N, D and S with $n = Le = 1$, $A^* = \xi = 0$. Table 4 lists the comparison of $-\theta'(\xi,0)$ for various values of n with $A^* = 1$, $N = D = S = \xi = 0$. Table 5 lists the comparison of $-\theta'(\xi,0)$ and $-\phi'(\xi,0)$ for various values of n and A^* with $D = S = 0$, $N = 4$, $Le = 10$. All values in Tables 1 to 5 list the comparisons showed excellent agreement with the numerical data in previous works.

Table 1. Comparison of $-\theta'(\xi,0)$ for various values of ξ with $N = D = S = A^* = 0, n = 1$.

ξ	$-\theta'(\xi,0)$				
	Minkowyez and Cheng [15]	Hooper et al. [16]	Yih [18]	Chamkha and Ben-Nakhi [22]	Present results
-4	2.0020	2.0015	2.0015	1.9989	2.0014
-2	1.0680	1.0725	1.0725	1.0726	1.0725
0	0.4438	0.4437	0.4437	0.4440	0.4437
2	0.1423	0.1417	0.1416	0.1424	0.1407
4	0.0335	0.0335	0.0333	0.0340	0.0329

Table 2. Comparison of $-\theta'(\xi,0)$ for various values of n and ξ with $N = D = S = A^* = 0$.

ξ	$-\theta'(\xi,0)$			
	$n = 0.5$		$n = 2.0$	
	Yih [19]	Present results	Yih [19]	Present results
-4	2.0001	2.0000	2.0094	1.9916
-2	1.0265	1.0267	1.1202	1.1164
0	0.3766	0.3765	0.4938	0.4937
2	0.1113	0.1107	0.1651	0.1648
4	0.0253	0.0247	0.0400	0.0398

Table 3. Comparison of $-\theta'(\xi,0)$ and $-\phi'(\xi,0)$ for various values of N, D and S with $n = Le = 1,\ A^* = \xi = 0.$

N	D	S	$-\theta'(\xi,0)$			$-\phi'(\xi,0)$		
			Tai and Char [6]	Postelnicu [28]	Present results	Tai and Char [6]	Postelnicu [28]	Present results
1	0.05	1.2	0.6767	0.6767	0.6767	0.1835	0.1835	0.1835
1	0.075	0.8	0.6510	0.6510	0.6510	0.3415	0.3415	0.3415
1	0.037	1.6	0.6968	0.6968	0.6968	0.0234	0.0233	0.0234
1	0.6	0.1	0.4200	0.4200	0.4200	0.6331	0.6331	0.6331
0.2	0.15	0.4	0.4633	0.4633	0.4633	0.3810	0.3810	0.3810

Table 4. Comparison of $-\theta'(\xi,0)$ for various values of n with $A^* = 1,\ N = D = S = \xi = 0$.

n	$-\theta'(\xi,0)$		
	Grosan and Pop [10]	Yih and Huang [12]	Present results
0.5	-0.2574	-0.2576	-0.2576
0.8	-0.2288	-0.2290	-0.2289
1.0	-0.2152	-0.2153	-0.2153
1.5	-0.1921	-0.1923	-0.1922
2.0	-0.1778	-0.1780	-0.1780
2.5	-0.1680	-0.1684	-0.1683

Table 5. Comparison of $-\theta'(\xi,0)$ and $-\phi'(\xi,0)$ for various values of A^* and n with $D=S=\xi=0$, $N=4$, $Le=10$

A^*	n	$-\theta'(\xi,0)$		$-\phi'(\xi,0)$	
		Yih and Huang [13]	Present results	Yih and Huang [13]	Present results
0	0.5	1.0105	1.0104	6.3671	6.3671
	1.0	0.6811	0.6810	3.2892	3.2892
	2.0	0.6030	0.6029	2.4022	2.4022
1	0.5	0.2404	0.2402	6.4412	6.4412
	1.0	-0.0191	-0.0191	3.3311	3.3311
	2.0	-0.0837	-0.0837	2.4247	2.4247

The numerical results are presented for the buoyancy ratio $N=2$, the Lewis number $Le=2$, the Dufour parameter $D=0.1$, the Soret parameter $S=0.2$, the internal heat generation A^* ranging from 0 to 1, the non-Newtonian fluid n ranging from 0.5 to 2.0, and the blowing/suction parameter ξ ranging from -2 to 2.

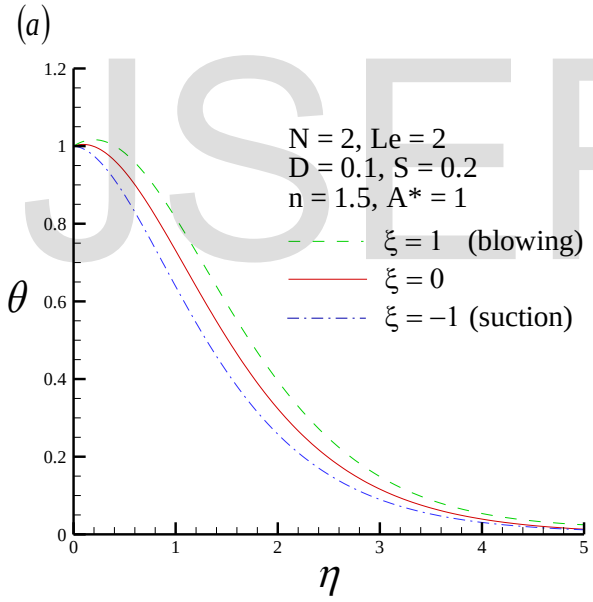

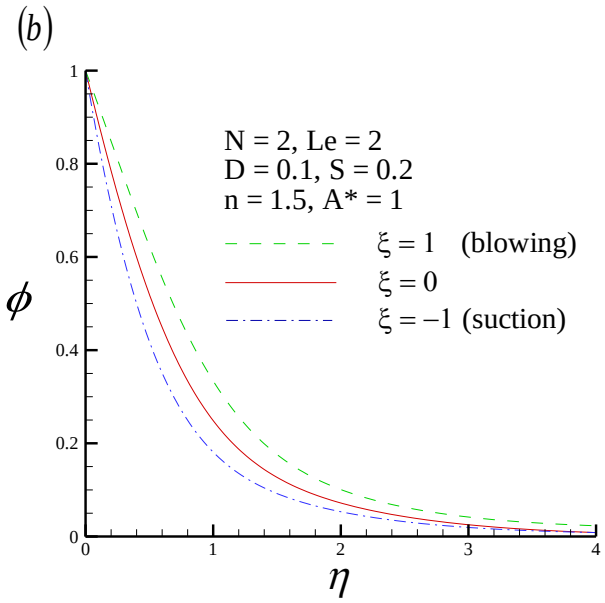

Fig. 2. (a) The dimensionless temperature profile and (b) the dimensionless concentration profile for three values of the blowing/suction parameter ξ.

Table 6. The values of $Nu_x / Ra_x^{1/2n}$ and $Sh_x / Ra_x^{1/2n}$ for various values of ξ with $N = 2$, $Le = 2$, $D = 0.1$, $S = 0.2$, $n = 1.5$, $A^* = 1$.

ξ	$Nu_x / Ra_x^{1/2n}$	$Sh_x / Ra_x^{1/2n}$
-2	0.1803	2.2768
-1	0.0179	1.6488
0	-0.0940	1.1289
1	-0.1677	0.7313
2	-0.2131	0.4479

Figure 2 portrays the dimensionless temperature and concentration profiles for three values of the blowing/suction parameter ξ ($\xi = -1$, 0 and 1) with $N = 2$, $Le = 2$, $D = 0.1$, $S = 0.2$, $n = 1.5$, $A^* = 1$, respectively. Figure 2(a) shows that case of blowing ($\xi > 0$) leads to a tendency to decrease the dimensionless wall temperature gradient $-\theta'(\xi,0)$. This phenomenon of overshoot in the dimensionless temperature profile is occurred for $\xi = 0$ and $\xi = 1$, where heat transfer is from the porous medium to the vertical flat plate. Moreover, Fig. 2(b) shows that case of suction $(\xi < 0)$ tends to increase the dimensionless wall concentration gradient $-\phi'(\xi,0)$. Both the thermal boundary layer thickness δ_T and the concentration boundary layer thickness δ_C increase for the case of blowing ($\xi > 0$). However, this trend is reversed in the case of suction ($\xi < 0$).

Table 6 lists the values of local Nusselt number $Nu_x / Ra_x^{1/2n}$ and the local Sherwood number $Sh_x / Ra_x^{1/2n}$ for various values of ξ with $N = 2$, $Le = 2$, $D = 0.1$, $S = 0.2$, $n = 1.5$ and $A^* = 1$. In general, it has been found that both the local Nusselt number and the local Sherwood number increase owing to the case of suction, i.e., $\xi < 0$. This is because for the case of suction increases both the dimensionless surface temperature and concentration gradients, as shown in Fig.

2. With the aid of Eqs. (26)-(27), the larger the dimensionless surface temperature and concentration gradients, the greater the local Nusselt and Sherwood numbers.

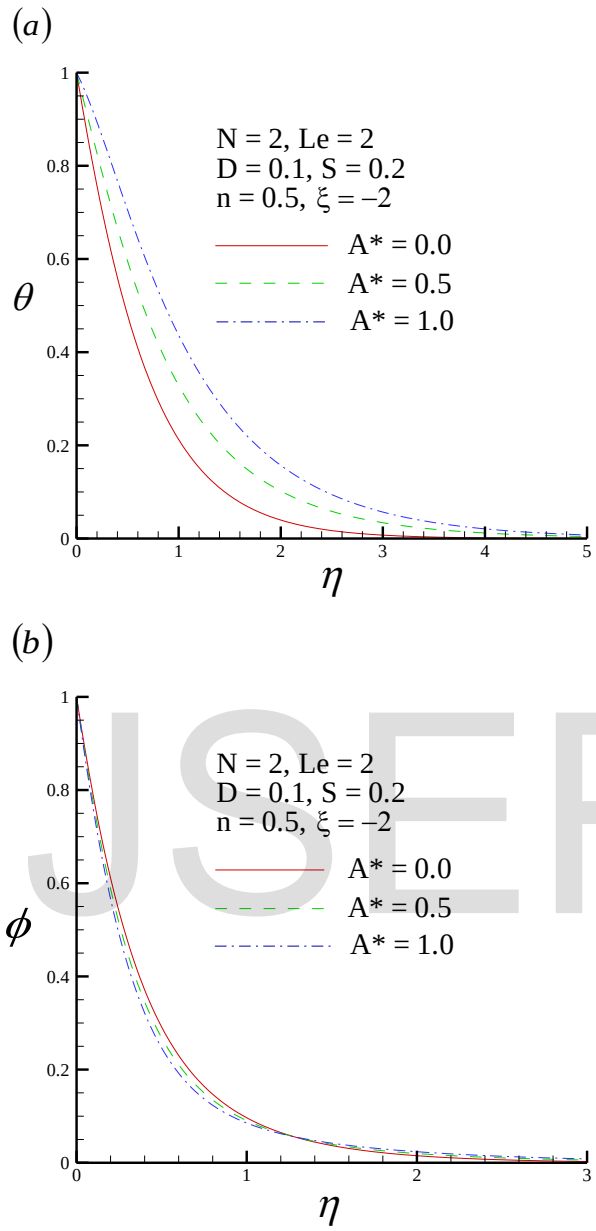

Fig. 3. (a) The dimensionless temperature profile and (b) the dimensionless concentration profile for three values of internal heat generation coefficient A^*.

Table 7. The values of $Nu_x / Ra_x^{1/2n}$ and $Sh_x / Ra_x^{1/2n}$ for various values of A^* with $N = 2,\ Le = 2,\ D = 0.1,\ S = 0.2,\ n = 0.5$ and $\xi = -2$.

A^*	$Nu_x / Ra_x^{1/2n}$	$Sh_x / Ra_x^{1/2n}$
0.0	1.3155	2.3813
0.25	1.0894	2.4756
0.50	0.8672	2.5680
0.75	0.6492	2.6584
1.0	0.4355	2.7468

The effect of the internal heat generation coefficient A^* ($A^* = 0.0,\ 0.5$ and 1.0) on the dimensionless temperature profile and the dimensionless concentration profile with $N = 2,\ Le = 2,\ D = 0.1,\ S = 0.2,\ n = 0.5$ and $\xi = -2$, is plotted in Fig. 3, respectively. It is observed that the increase of the internal heat generation coefficient A^* leads to a tendency to decrease the dimensionless wall temperature gradient $-\theta'(\xi,0)$ but increase the dimensionless wall concentration gradient $-\phi'(\xi,0)$.

Table 7 lists the values of local Nusselt number $Nu_x / Ra_x^{1/2n}$ and the local Sherwood number $Sh_x / Ra_x^{1/2n}$ for various values of the internal heat generation coefficient A^* with $N = 2,\ Le = 2,\ D = 0.1,\ S = 0.2,\ n = 0.5$ and $\xi = -2$. In general, it has been found that enhancing the internal heat generation coefficient A^* reduces the local Nusselt number and enhances slightly the local Sherwood number. This is due to the fact that enhancing the internal heat generation coefficient A^* tends to decreases the dimensionless surface temperature gradients and increases the dimensionless surface concentration gradients, as shown in Fig. 3, thus lowering the local Nusselt number and highering the local Sherwood number.

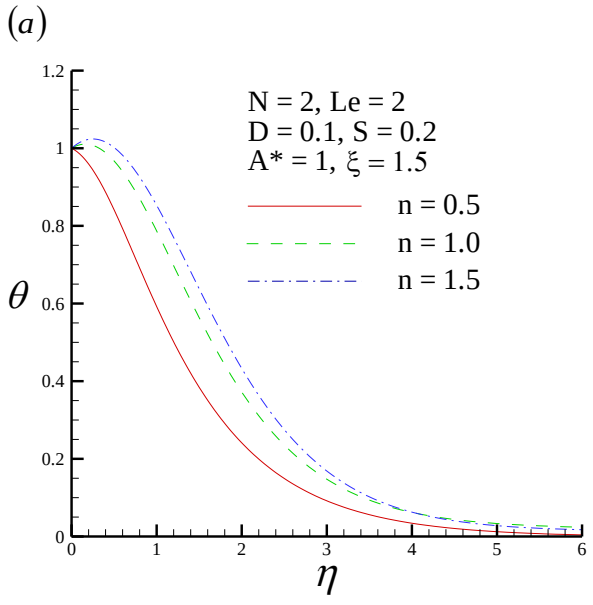

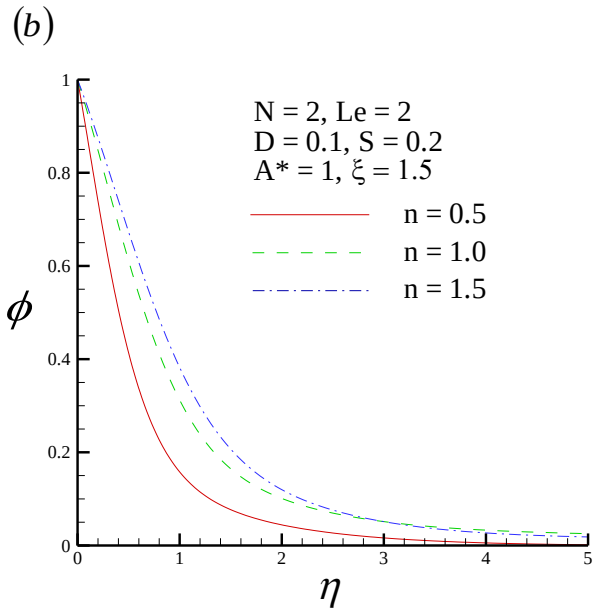

Fig. 4. (a) The dimensionless temperature profile and (b) the dimensionless concentration profile for three values of the non-Newtonian fluid n.

Table 8. The values of $Nu_x / Ra_x^{1/2n}$ and $Sh_x / Ra_x^{1/2n}$ for various values of n with $N = 2,\ Le = 2,\ D = 0.1,\ S = 0.2,\ \xi = 1.5$ and $A^* = 1$.

n	$Nu_x / Ra_x^{1/2n}$	$Sh_x / Ra_x^{1/2n}$
0.5	0.1096	1.2398
0.8	-0.0804	0.8133
1.0	-0.1316	0.7029
1.5	-0.1933	0.5765
2.0	-0.2216	0.5216

Figure 4 portrays the dimensionless temperature and concentration profiles for three values of the non-Newtonian fluid n ($n = 0.5, 1.0$ and 1.5) with $N = 2$, $Le = 2$, $D = 0.1$, $S = 0.2$, $\xi = 1.5$, $A^* = 1$, respectively. It is obviously found that the dimensionless temperature profiles $\theta(\xi,\eta)$ and the dimensionless concentration profiles $\phi(\xi,\eta)$ decrease with decreasing the non-Newtonian fluid n, thus decreasing the thermal and concentration boundary layer thicknesses. This is because decreasing the non-Newtonian fluid n tends to increase the buoyancy force and the flow velocity.

Table 8 lists the values of local Nusselt number $Nu_x / Ra_x^{1/2n}$ and the local Sherwood number $Sh_x / Ra_x^{1/2n}$ for various values of the non-Newtonian fluid n with $N = 2$, $Le = 2$, $D = 0.1$, $S = 0.2$, $\xi = 1.5$ and $A^* = 1$. It is also found that enhancing the non-Newtonian fluid n reduces both the local Nusselt number and the local Sherwood number. This is because enhancing the non-Newtonian fluid n tends to retard the velocity of the flow and reduces the dimensionless surface temperature and concentration gradients, as shown in Fig. 4. Therefore pseudoplastic fluids (n = 0.5) are superior to the dilatant fluids (n = 1.5) from the viewpoint of the heat and mass transfer

rates by natural convection from a vertical plate embedded in a porous medium saturated with non-Newtonian power-law fluids.

5. Conclusions

A two-dimensional laminar boundary layer analysis is presented to study the influence of uniform blowing/suction on the natural convection of non-Newtonian fluids over a vertical plate in porous media with internal heat generation and Soret/Dufour effects. After the coordinate transformation, the transformed governing equations are solved by Keller box method (KBM). Comparisons with previously published works show excellent agreement. Numerical solutions are obtained for different values of the internal heat generation coefficient A^*, the power-law index of the non-Newtonian fluid n and the blowing/suction parameter ξ. Results show that increasing the internal heat generation coefficient A^* tends to reduce the local Nusselt number and enhance the local Sherwood number. Otherwise, when the power-law index of non-Newtonian fluid n increases, both the local Nusselt number and the local Sherwood number decrease. In general, for the case of suction, both the local Nusselt number and the local Sherwood number increase. This trend reversed for blowing of fluid.

References

[1] D.A. Nield, A. Bejan, Convection in Porous Media, Springer-Verlag, New York (2006).

[2] H.T. Chen, C.K. Chen, Natural convection of a non-Newtonian fluid about a horizontal cylinder and a sphere in a porous medium, International Communications in Heat and Mass Transfer 15(5) (1988), 605–614.

[3] S.K. Rastogi, D. Poulikakos, Double-diffusion from a vertical surface in a porous region saturated with a non-Newtonian fluid, International Journal of Heat and Mass Transfer 38(5) (1995), 935–946.

[4] R.Y. Jumah, A.S. Mujumdar, Natural convection heat and mass transfer from a vertical flat plate with variable wall temperature and concentration to power-law fluids with yield stress in a porous medium, Chemical Engineering Communications 185(1) (2001), 165–182.

[5] C.Y. Cheng, Natural convection heat and mass transfer of non-Newtonian power law fluids with yield stress in porous media from a vertical plate with variable wall heat and mass fluxes, International Communications in Heat and Mass Transfer 33(9) (2006), 1156–1164.

[6] B.C. Tai, M.I. Char, Soret and Dufour effects on free convection flow of non-Newtonian fluids along a vertical plate embedded in a porous medium with thermal radiation, International Communications in Heat and Mass Transfer 37 (2010), 480–483.

[7] S. Bagai, C. Nishad, Free convection in a non-Newtonian fluid along a horizontal plate embedded in porous media with internal heat generation, International Communications in Heat and Mass Transfer 39(4) (2012), 537–540.

[8] J.C. Crepeau, R. Clarksean, Similarity solutions of natural convection with internal heat generation, Journal of Heat Transfer 119 (1997), 183–184.

[9] A. Postelnicu, I. Pop, Similarity solutions of free convection boundary layers over vertical and horizontal surfaces in porous media with internal heat generation, International Communications in Heat and Mass Transfer 26(8) (1999), 1183–1191.

[10] T. Grosan, I. Pop, Free convection over a vertical flat plate with a variable wall temperature and internal heat generation in a porous medium saturated with a non-Newtonian fluid, Technische Mechanik 21(4) (2001), 313–318.

[11] T. Grosan, A. Postelnicu, I. Pop, Free convection boundary layer over a vertical cone in a non-Newtonian fluid saturated porous medium with internal heat generation, Technische Mechanik 24 (2004), 91–104.

[12] P.M. Patil, S. Roy, I. Pop, Flow and heat transfer over a moving vertical plate in a parallel free stream: role of internal heat generation or absorption, Chemical Engineering Communications 199(5) (2012), 658–672.

[13] K.A. Yih, C.J. Huang, Effect of internal heat generation on free convection heat and mass transfer of non-Newtonian fluids flow over a vertical plate in porous media: VWT/VWC, Journal of Aeronautics, Astronautics and Aviation 47(2) (2015), 115–122.

[14] K.A. Yih, C.J. Huang, Effect of internal heat generation on free convection flow of non-Newtonian fluids over a vertical truncated cone in porous media: VWT/VWC, Journal of Air Force Institute of Technology 14(1), (2015), 1–18.

[15] W.J. Minkowycz, P. Cheng, Local non-similar solutions for free convective flow with uniform lateral mass flux in porous medium, Letters in Heat and Mass Transfer 9(3) (1982), 159–168.

[16] W.B. Hooper, T.S. Chen, B.F. Armaly, Mixed convection from a vertical plate in porous media with surface injection or suction, Numerical Heat Transfer, Part A: Applications 25(3) (1994), 317–329.

[17] Y.T. Yang, S.J. Wang, Free convection heat transfer of non-Newtonian fluids over axisymmetric and two-dimensional bodies of arbitrary shape embedded in a fluid-saturated porous medium, International Journal of Heat and Mass Transfer 39(1) (1996), 203–210.

[18] K.A. Yih, The effect of uniform lateral mass flux on free convection about a vertical cone embedded in a saturated porous medium, International Communications in Heat and Mass Transfer 24(8) (1997), 1195–1205.

[19] K.A. Yih, Uniform lateral mass flux effect on natural convection of non-Newtonian fluids over a cone in porous media, International Communications in Heat and Mass Transfer 25(7) (1998), 959–968.

[20] F.S. Ibrahim, M.A. Mansour, S.M. Abdel-Gaied, Radiative and thermal dispersion effects on non-Darcy natural convection with lateral mass flux for non-Newtonian fluid from a vertical flat plate in a saturated porous medium, Transport in porous media 61 (2005), 45–57.

[21] M.E. Ali, The effect of lateral mass flux on the natural convection boundary layers induced by a heated vertical plate embedded in a saturated porous medium with internal heat generation, International Journal of Thermal Sciences 46 (2007), 157–163.

[22] A.J. Chamkha, A. Ben-Nakhi, MHD mixed convection–radiation interaction along a

permeable surface immersed in a porous medium in the presence of Soret and Dufour's Effects, Heat and Mass Transfer 44 (2008), 846–856.

[23] M. Kumari, G. Nath, Natural convection from a vertical cone in a porous medium due to the combined effects of heat and mass diffusion with non-uniform wall temperature/concentration or heat/mass flux and suction/injection, International Journal of Heat and Mass Transfer 52(13–14) (2009), 3064–3069.

[24] A.M. Rashad, M.A. EL-Hakiem, M.M.M. Abdou, Natural convection boundary layer of a non-Newtonian fluid about a permeable vertical cone embedded in a porous medium saturated with a nanofluid, Computers and Mathematics with Applications 62(8) (2011), 3140–3151.

[25] R.V. Christopher, S. Middleman, Power-law Flow through a Packed Tube, Industry and Engineering Chemistry Fundamentals 4(4) (1965), 424–426.

[26] R.V. Dharmadhirkari, D.D. Kale, Flow of non-Newtonian Fluids through Porous Media, Chemical Engineering Science 40(3) (1985), 527–529.

[27] T. Cebeci, P. Bradshaw, Physical and Computational Aspects of Convective Heat Transfer, Springer-Verlag, New York (1984), 385.

[28] A. Postelnicu, Influence of a magnetic field on heat and mass transfer by natural convection from vertical surfaces in porous media considering Soret and Dufour effects, International Journal of Heat and Mass Transfer 47 (2004), 1467–1472.